

# EPJ E

Soft Matter and  
Biological Physics

EPJ.org  
your physics journal

Eur. Phys. J. E (2013) **36**: 25

DOI 10.1140/epje/i2013-13025-0

## Phason-induced dynamics of colloidal particles on quasicrystalline substrates

Justus A. Kromer, Michael Schmiedeberg, Johannes Roth and Holger Stark

edp sciences



Springer

# Phason-induced dynamics of colloidal particles on quasicrystalline substrates

Justus A. Kromer<sup>1</sup>, Michael Schmiedeberg<sup>2,a</sup>, Johannes Roth<sup>3</sup>, and Holger Stark<sup>4</sup>

<sup>1</sup> Institut für Physik, Humboldt-Universität zu Berlin, Newtonstraße 15, D-12489 Berlin, Germany

<sup>2</sup> Institut für Theoretische Physik 2: Weiche Materie, Heinrich-Heine-Universität Düsseldorf, D-40204 Düsseldorf, Germany

<sup>3</sup> Institut für Theoretische und Angewandte Physik, Universität Stuttgart, Pfaffenwaldring 57, D-70550 Stuttgart, Germany

<sup>4</sup> Institut für Theoretische Physik, Technische Universität Berlin, Hardenbergstr. 36, D-10623 Berlin, Germany

Received 4 December 2012 and Received in final form 15 February 2013

Published online: 21 March 2013 – © EDP Sciences / Società Italiana di Fisica / Springer-Verlag 2013

**Abstract.** Phasons are special hydrodynamic modes that occur in quasicrystals. The trajectories of particles due to a phasonic drift were recently studied by Kromer *et al.* (Phys. Rev. Lett. **108**, 218301 (2012)) for the case where the particles stay in the minima of a quasicrystalline potential. Here, we study the mean motion of colloidal particles in quasicrystalline laser fields when a phasonic drift or displacement is applied and also consider the cases where the colloids cannot follow the potential minima. While the mean square displacement is similar to the one of particles in a random potential with randomly changing potential wells, there also is a net drift of the colloids that reverses its direction when the phasonic drift velocity is increased. Furthermore, we explore the dynamics of the structural changes in a laser-induced quasicrystal during the rearrangement process that is caused by a steady phasonic drift or an instantaneous phasonic displacement.

## 1 Introduction

Quasicrystals are not periodic in space but still possess long-ranged positional order [1,2]. A special feature of quasicrystals are the so-called phasons, which are hydrodynamic modes that like phonons do not change the free energy in the long wavelength limit [3]. The properties of phasons in atomic quasicrystals are a major topic of research and discussions [4,5]. Recently, the motion of particles due to a phasonic drift was revealed by studying the trajectories of colloids in a laser field with quasicrystalline symmetry [6,7].

Colloidal particles in external fields are a widely studied system in statistical physics [8]. Especially by applying a laser field to a two-dimensional colloidal suspension, the colloidal particles are forced into the regions of largest laser intensity [9,10]. Therefore, a laser field acts like a substrate or external potential and can be employed to obtain colloidal structures with the same symmetry as the laser field [11]. For example, by using the interference patterns of five, seven, or more laser beams, light-induced colloidal quasicrystals are obtained. They are widely used as a model system to study the behavior of particles on quasicrystalline substrates, *e.g.*, to explore the ordering of the particles [12–16], their dynamics [17–20], or in order to answer fundamental questions related to the stability [21,22] or frictional properties [23] of quasicrystals.

The collective rearrangements due to a phasonic displacement were demonstrated in [13] for a decagonal phase and in [15] for an Archimedean tiling-like ordering.

For a quasicrystalline substrate with phasonic drift, *i.e.* for the case where the phasonic displacement is increased at a constant rate in time, the trajectories of the colloidal particles can be predicted in the limit of slow phasonic drifts, small friction, and at low temperatures or large laser intensities [6,7]. In this limit the colloid follows the positions of the minima of the external potential that is created by the laser field. Only when a minimum disappears, the colloidal particle slides into a potential well nearby. The colloidal path is determined by the behavior of a particle within characteristic areas of reduced phononic and phasonic displacement [6,7]. Therefore, only a few types of trajectories occur, *e.g.*, for a phasonic drift in the  $x$ -direction some colloids move on straight paths to the right (red particles in fig. 1(a)) while the other follow zigzag trajectories to the left (depicted green in fig. 1(a)). For a phasonic drift in the  $y$ -direction the colloids move on zigzag paths either from top to bottom or from bottom to top (fig. 1(b), shown in brown and magenta, respectively).

For large phasonic drift velocities, a large friction constant, or a small potential strength, the colloidal particles cannot follow the motion of the minima of the substrate. Furthermore, at a finite temperature a colloid might jump from one potential well into another one. Therefore, the colloidal particle does not follow deterministic trajectories.

<sup>a</sup> e-mail: schmiedeberg@thphy.uni-duesseldorf.de

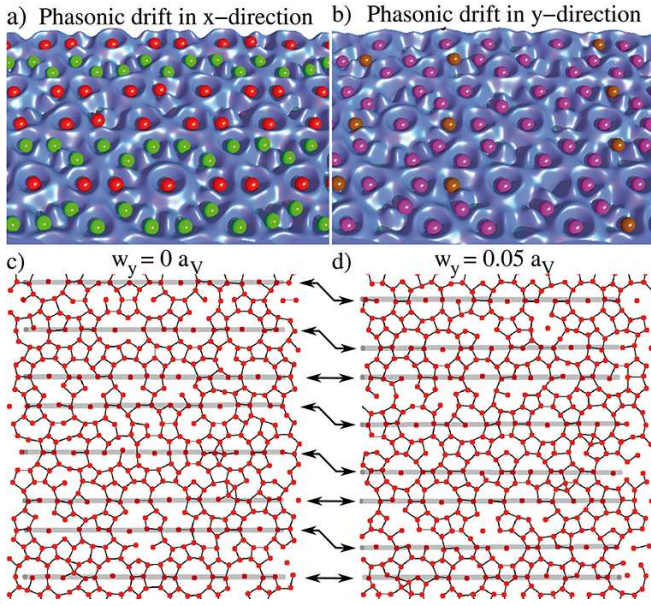


**Fig. 1.** Colloidal particles on a decagonal substrate. (a) For a phasonic drift in the  $x$ -direction the red particles move on straight trajectories to the right, the green particles follow a zigzag path to the left. (b) For a phasonic drift in the  $y$ -direction, all particles move on zigzag trajectories. The brown colloids head from top to bottom, the magenta ones move in the opposite direction (cf. [6]). (c,d) Snapshots of a laser-induced colloidal quasicrystal (c) before and (d) after a phasonic displacement in the  $y$ -direction. The gray areas indicate the lines of symmetry centers. The sequence of the distances between these lines is altered by the phasonic displacement.

In this article, we study the average motion of colloidal particles in a substrate with phasonic drift beyond the limits considered in [6, 7].

We also study how phasonic displacements or drifts affect laser-induced decagonal colloidal quasicrystals. As shown in fig. 1(c,d), a phasonic displacement enforces a rearrangement of the colloidal particles. For example, some lines of local symmetry centers are displaced to a new location. We determine how the quasicrystalline order is restored after an instantaneous phasonic displacement and analyze the colloidal structure on a decagonal substrate with a steady phasonic drift.

The article is organized as follows. In sect. 2 we introduce the model and describe the details of our Brownian dynamics simulations. In sect. 3 the motion of single particles in a potential with constant phasonic drift is described while in sect. 4 the rearrangement process of a light-induced quasicrystal due to a phasonic drift or a phasonic displacement is studied. Finally, we conclude in sect. 5.

## 2 Model system and simulation details

We consider a charged-stabilized colloidal suspension that is subjected to a laser field. The colloids are forced into the areas with the largest laser intensity [9–11]. To obtain

a laser field with decagonal quasicrystalline symmetry, we consider the interference pattern of five laser beams, which corresponds to an external potential given by [24, 17]

$$V(\mathbf{r}) = -\frac{V_0}{25} \sum_{j=0}^4 \sum_{k=0}^4 \cos[(\mathbf{G}_j - \mathbf{G}_k) \cdot \mathbf{r} + \phi_j - \phi_k], \quad (1)$$

where  $\mathbf{G}_j = (2\pi \cos[2\pi j/5]/a_V, 2\pi \sin[2\pi j/5]/a_V)$  are the wave vectors projected onto the  $xy$ -plane,  $a_V$  is the length scale of the potential, and  $\phi_j$  are the phases of the laser beams. In experiments the corresponding laser field can be obtained by splitting a laser beam into five parts. The five beams then are focused onto the sample in a way that is symmetric with respect to the direction perpendicular to the sample cell (cf. [14, 16]). The phasonic displacement  $\mathbf{u} = (u_x, u_y)$  and the phasonic displacement  $\mathbf{w} = (w_x, w_y)$  are realized by choosing the phases according to [3]

$$\phi_j = \mathbf{u} \cdot \mathbf{G}_j + \mathbf{w} \cdot \mathbf{G}_{3j \bmod 5}. \quad (2)$$

In experiments only four phases have to be controlled simultaneously because the global phase does not change the potential. In the following we either consider a phasonic drift, where the phasonic displacement is increased at a constant rate in time, or we assume a constant global phasonic displacement  $\mathbf{w}$  that does not depend on position and is switched on instantaneously.

In sect. 4 we consider colloidal particles which interact by the pair potential  $\phi(r_{ij})$  of the Derjaguin-Landau-Verwey-Overbeek-theory [25, 26]

$$\phi(r_{ij}) = \frac{(Z^* e)^2}{2\pi\epsilon_0\epsilon_r} \left( \frac{e^{\kappa R}}{1 + \kappa R} \right)^2 \frac{e^{-\kappa r_{ij}}}{r_{ij}}, \quad (3)$$

where  $r_{ij} = |\mathbf{r}_i - \mathbf{r}_j|$  is the distance between colloid  $i$  and  $j$ .  $R$  is the radius of a colloid,  $Z^*$  its effective surface charge,  $\epsilon_r$  the dielectric constant of water, and  $\kappa$  the inverse Debye screening length. We employ the same parameters as for the high density simulations in [13], *i.e.*,  $R = 1.2 \mu\text{m}$ ,  $Z^* = 1000$ ,  $\epsilon_r = 78$ , and  $\kappa^{-1} = 0.25 \mu\text{m} = a_V/20$ , where  $a_V = 5.0 \mu\text{m}$ .

In order to quantify the amount of quasicrystalline order, we calculate the bond orientational order parameter

$$\Psi_{10} = \left\langle \left| \frac{1}{N} \sum_{j=1}^N \frac{1}{n_j} \sum_{k=1}^{n_j} e^{10i\theta_{jk}} \right| \right\rangle, \quad (4)$$

where  $\theta_{jk}$  is the angle of the bond between particles  $j$  and  $k$  with respect to some arbitrary reference direction and the outer sum is over all  $N$  particles while the inner sum is over the  $n_j$  nearest neighbors of colloid  $j$ . The nearest neighbors are determined with a Voronoi construction. The bond orientational order parameter  $\Psi_{10}$  is nonzero in a quasicrystal with ten bond directions but zero in a disordered phase. A detailed analysis of the phase behavior of a laser-induced colloidal quasicrystal on a decagonal substrate using the bond orientational order parameter is presented in [13].

We perform Brownian dynamics simulations, *i.e.*, we solve the overdamped Langevin equation

$$\gamma \frac{d}{dt} \mathbf{r}_j = -\nabla \sum_i \phi(|\mathbf{r}_i - \mathbf{r}_j|) - \nabla V(\mathbf{r}_j) + \mathbf{f}(t), \quad (5)$$

where  $\mathbf{r}_j$  denotes the position of the  $j$ -th colloid and  $\gamma$  its friction coefficient. The interaction potential is given in eq. (3) and the external potential  $V(\mathbf{r})$  by eq. (1). The thermal force  $\mathbf{f}(t)$  is realized by random kicks with zero mean,  $\langle \mathbf{f}(t) \rangle = 0$ , and two-point correlations given by the fluctuation-dissipation theorem

$$\langle f_i(t) f_j(t') \rangle = 2\gamma k_B T \delta_{ij} \delta(t - t'). \quad (6)$$

The initial positions of the colloids are chosen randomly.

To study colloidal quasicrystals in sect. 4, we use periodic boundary conditions and the system size is always chosen such that it best suits the quasicrystalline order (cf. [13]).

### 3 Single colloids on a substrate with phasonic drift

First, we consider the dynamics of a single colloidal particle in a potential where a constant phasonic drift is applied, *i.e.*, the phasonic displacement is changed at a constant rate in time.

#### 3.1 Mean square displacement of the colloidal particles

We calculate the mean squared displacement of the colloidal positions that is corrected by the mean drift motion, *i.e.*

$$\langle r^2(t) \rangle = \langle |\mathbf{r}(t) - \langle \mathbf{r}(t) \rangle|^2 \rangle, \quad (7)$$

where the average is an ensemble average over 2000 particles with different random starting positions. In fig. 2 the mean square displacement is shown for different phasonic drift velocities  $dw_x/dt$ . Without phasonic drift ( $|d\mathbf{w}/dt| = 0$ ), the mean square displacement crosses over from the initial diffusive or slightly superdiffusive motion within a potential well to an extended intermediate subdiffusive regime where the colloids jump between neighboring minima but have not yet explored the whole potential. In the long-time limit, we expect a crossover into the asymptotic diffusive regime. This behavior already has been studied in [17]. For increasing phasonic drift velocity, the subdiffusive regime becomes shorter and the diffusion constant at long times increases. For a large phasonic drift velocity the asymptotic long-time behavior is similar to free diffusion of the particles without potential, which is shown in fig. 2 by the red curve.

In order to gain a deeper understanding of the behavior described above, we will shortly describe in the next subsection how the random trap model developed in [17] can be modified such that it qualitatively predicts the time dependence of the mean square displacement.

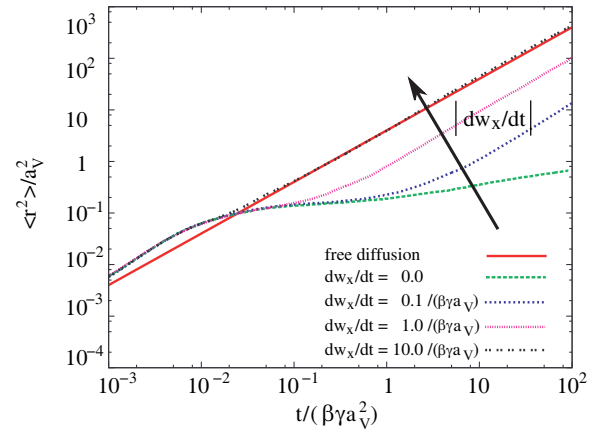


**Fig. 2.** Mean square displacement of colloidal particles in a decagonal potential whose phasonic displacement in the  $x$ -direction is increased at different rates in time  $dw_x/dt$ . The strength of the potential is  $V_0 = 20k_B T$ , time is plotted in units of the diffusive time scale  $\beta \gamma a_V^2$ , where  $\beta = (k_B T)^{-1}$  is the inverse temperature,  $\gamma$  is the friction coefficient, and  $a_V$  denotes the length scale of the potential (cf. sect. 2). For comparison, the red curve shows the mean square displacement of freely diffusing colloids without external potential.

#### 3.2 Random trap model for non-equilibrium

The diffusive motion of a colloid in the quasicrystalline potential can be described by a random trap model where a minimum is seen as a trapping site for the particle [17]. The probability to leave a minimum and jump into a neighboring one is given by a transition rate  $\Gamma(V_m)$  that can be determined by Kramer's formula [27] and depends on the depth  $V_m$  of the minimum. We introduce the probability distribution  $P(V_m, t) dV_m$  for the probability that the colloid at time  $t$  is in a minimum of depth  $V_m$ . In a static quasicrystalline or random potential, *i.e.*, without phasonic drift a rate equation for  $P(V_m, t)$  can be derived. The change of the probability for the colloid to occupy a minimum of depth  $V_m$  is [17]

$$\begin{aligned} \frac{d}{dt} P(V_m, t) = & -z\Gamma(V_m)P(V_m, t) \\ & + z\rho(V_m) \int_0^{V_0} dV'_m \Gamma(V'_m) P(V'_m, t), \end{aligned} \quad (8)$$

where  $z$  is the number of neighboring minima and  $\rho(V_m)$  is the probability that a minimum of the potential has the depth  $V_m$ . The first term on the right-hand side denotes the probability to leave a minimum while the second term corresponds to the averaged probability that a colloid from any neighboring minimum jumps into the potential well. The rate eq. (8) can be solved numerically, *i.e.*, for a given starting configuration  $P(V_m, t = 0)$  the probability  $P(V_m, t)$  can be determined at all times  $t$ . Furthermore, the time-dependent diffusion constant  $D(t) = \frac{d}{dt} \langle r^2(t) \rangle / 4$  is [17]

$$D(t) = \frac{z l^2}{4} \int_0^{V_0} dV_m \Gamma(V_m) P(V_m, t). \quad (9)$$

In a quasicrystalline potential that is subjected to a constant phasonic drift, the depth of a minimum is changing with time. Therefore, we modify the random trap model accordingly. For simplicity, we assume that the depth  $V_m$  decreases or increases as in a one-dimensional random walk. Then,  $P(V_m, t)$  does also change if the depth of a shallower minimum increases, the depth of a deeper minimum decreases or the considered minimum itself changes its depth. Therefore, due to the phasonic drift, there is an additional contribution to  $\frac{d}{dt}P(V_m, t)$  that is proportional to

$$P(V_m - dV_m, t) + P(V_m + dV_m, t) - 2P(V_m, t) \propto \frac{d^2}{dV_m^2} P(V_m, t). \quad (10)$$

As a consequence, we obtain an extended rate equation

$$\begin{aligned} \frac{d}{dt}P(V_m, t) = & -z\Gamma(V_m)P(V_m, t) \\ & + z\rho(V_m) \int_0^{V_0} dV'_m \Gamma(V'_m)P(V'_m, t) \\ & + D_w \frac{d^2}{dV_m^2} P(V_m, t), \end{aligned} \quad (11)$$

where  $D_w$  denotes the rate, at which the minima change their depth. Therefore,  $D_w$  is a parameter similar to the phasonic drift velocity that controls the rate of changes of the quasicrystalline substrate in the simulations.

We solved (11) numerically for the case where the initial  $P(V_m, t = 0)$  is given by the probability that a minimum of depth  $V_m$  occurs in the decagonal potential. This corresponds to colloidal particles starting at random positions. At long times,  $P(V_m, t)$  enters a stationary state, *i.e.*,  $\frac{d}{dt}P(V_m, t) = 0$ . In fig. 3(a) this long-time limit of  $P(V_m, t)$  is shown for different values of  $D_w$ . For  $D_w = 0$ , (11) leads to

$$P(V_m, t \rightarrow \infty) = \frac{\frac{\rho(V_m)}{\Gamma(V_m)}}{\int_0^{V_0} dV'_m \frac{\rho(V'_m)}{\Gamma(V'_m)}}, \quad (12)$$

which can also be derived from a Boltzmann distribution of the particles. For  $D_w > 0$ , the probability to occupy shallower minima increases. This is due to a steady energy influx that drives the system out of equilibrium.

In fig. 3(b) the mean square displacement is shown calculated by integrating the diffusion constant that is determined using (9). We find a crossover from a sub diffusive to a diffusive regime for all values of  $D_w$ . Note, there is no diffusive regime for short times as in the simulations (fig. 2), because the random trap model does not take into account the motion of a particle within a potential minimum. However, the random trap model predicts the subdiffusive regime for intermediate times and the diffusive regime at long times. In particular, for increasing  $D_w$  the crossover into the diffusive long-time regime occurs earlier. Furthermore, the effective diffusion constant increases. Therefore, the modified random trap model correctly describes the

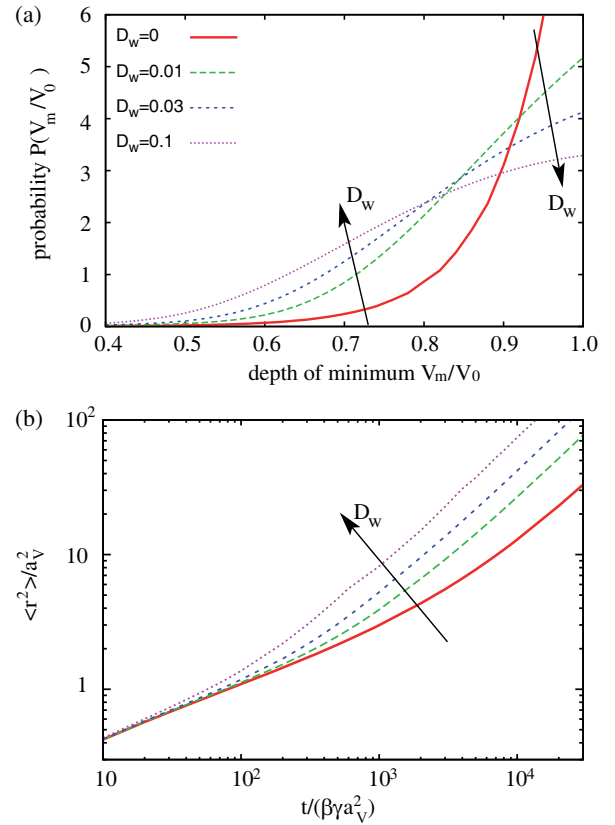


**Fig. 3.** Results of the random trap model calculations. (a) Probability to find a particle in a minimum of depth  $V_m/V_0$ . (b) Mean square displacement depending on time. The parameter  $D_w$  describes the rate at which the depth of the minima are changing. A large value of  $D_w$  corresponds to a large phasonic drift.

qualitative behavior of a colloidal particle in a quasicrystalline potential with a constant phasonic drift. Obviously, the phasonic drift drives the colloids out of equilibrium which leads to a diffusive regime that starts earlier and possesses a larger effective diffusion constant. Therefore, colloids in a quasicrystalline potential can be used to study non-equilibrium dynamics similar to driven particles in tilted potentials (see, *e.g.* [28–31]).

Note that in (7) we considered the mean square displacement  $\langle r^2(t) \rangle$  that is corrected by the mean colloidal drift motion. As we will show in the next section, a phasonic drift also induces a net drift of the colloidal particles. This colloidal drift cannot be predicted by assuming uncorrelated random changes of the depths of the potential wells. Therefore, while the qualitative behavior of the mean square displacement can be correctly described by the modified random trap model, the drift of the colloids cannot.

### 3.3 Mean drift velocity and direction of the colloidal particles

Figure 4(a) depicts the mean colloidal displacement in the  $x$ -direction for a particle that was at the origin at

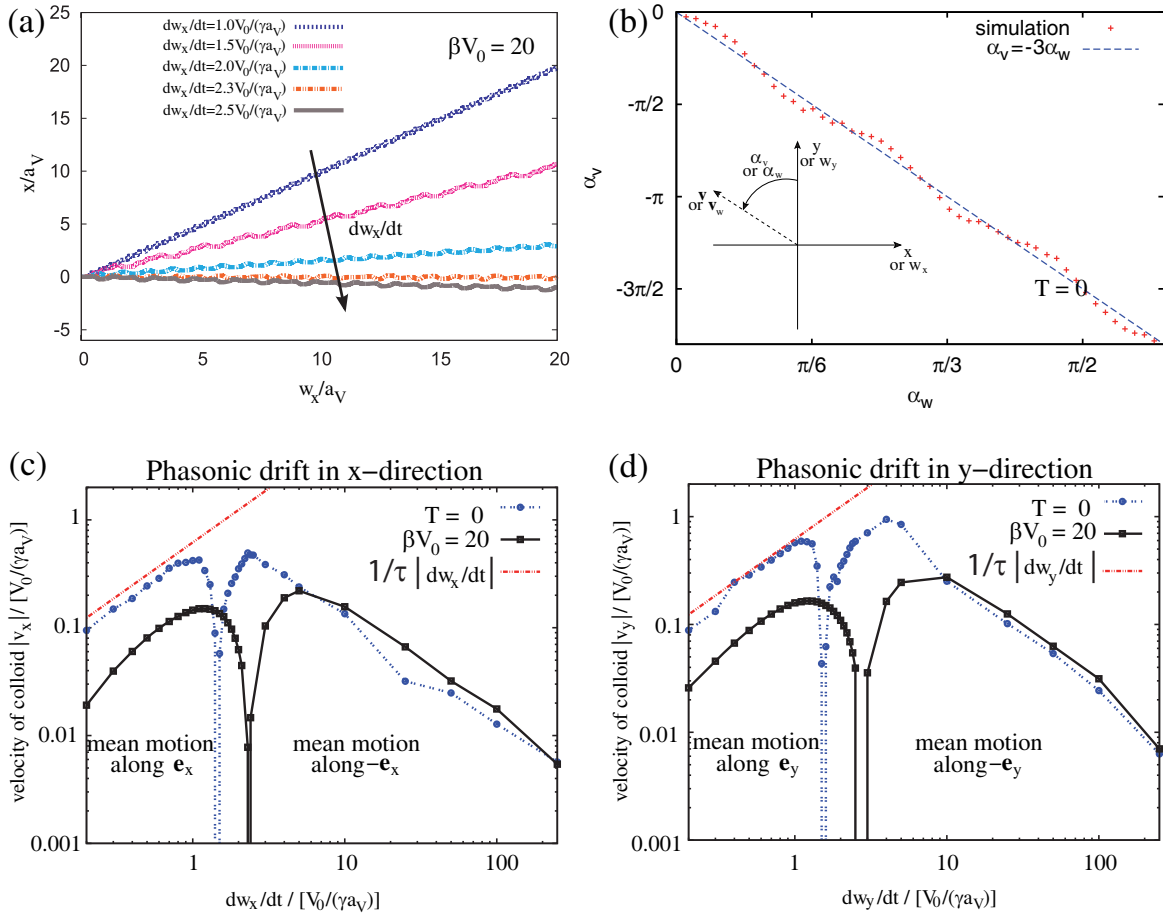


**Fig. 4.** (a) Mean displacement  $x$  of the colloidal particles that were started at the origin as a function of the phasonic displacement  $w_x$  for different phasonic drift velocities  $dw_x/dt$ . (b) Direction of the colloidal drift measured by the angle  $\alpha_v$  as a function of the phasonic drift direction given by  $\alpha_w$  for a small phasonic drift velocity  $|d\mathbf{w}/dt| = 5 \cdot 10^{-4} V_0/(\gamma a_V)$ . The angles are defined with respect to the  $y$ -direction as shown in the inset. The simulation results are close to  $\alpha_v = -3\alpha_w$  (blue line). (c,d) Mean colloidal velocity for particles started at random positions plotted *versus* the phasonic drift velocities for a phasonic drift in (c)  $x$ -direction and (d)  $y$ -direction. On the left branches of the curves the mean drift of the colloids is in the direction of the phasonic drift, on the right branches it is in the opposite direction. The blue lines denote the zero-temperature simulations while the black lines are obtained at a finite temperature  $k_B T = V_0/20$ . The red lines show  $|\mathbf{v}| = |d\mathbf{w}/dt|/\tau$ , with  $\tau = (1 + \sqrt{5})/2$  for comparison.

time  $t = 0$  as a function of the phasonic displacement  $w_x$ . Such a particle follows a trajectory that is typical for the colloids shown in red in fig. 1(a). We observe a net drift motion in the  $x$ -direction of the colloidal particles for small  $dw_x/dt$ . Interestingly for increasing  $dw_x/dt$  the drift becomes smaller and even changes its direction for large  $dw_x/dt$ .

In fig. 4(c) and (d) the absolute value of the mean colloidal drift velocities in  $x$ - and  $y$ -direction are shown as a function of the phasonic drift velocities  $dw_x/dt$  and  $dw_y/dt$ , respectively. The colloids are started at random initial positions and the results are averaged over 2000 runs. Note that for a small phasonic drift the colloidal particles on average move in  $+x$ -direction for a phasonic drift in  $x$ -direction and in  $+y$ -direction for a phasonic drift in  $y$ -direction. However, for a large phasonic drift the net drift is in the opposite direction. The details of this behavior

can best be analyzed in the zero-temperature limit. We observe that for  $|d\mathbf{w}/dt| < V_0/(2\gamma a_V)$  almost all particles follow the position of the minima as described in [6]. This corresponds to the limit of small friction  $\gamma$  or large potential strength  $V_0$ . For  $|d\mathbf{w}/dt| \approx V_0/(2\gamma a_V)$  some of the colloids can no longer follow the modulation of the potential. Specifically, particles in shallow minima no longer contribute to the net motion while colloids in deep wells still possess the same trajectory as in the case of small phasonic drift. For a phasonic drift in the  $x$ -direction, the particles depicted red in fig. 1(a) usually occupy deeper minima than the colloids shown in green. Since the red particles move on straight paths and the green colloids along zigzag trajectories in the opposite direction [6], the mean drift in  $+x$ -direction increases slightly more than linear if the green particles cease to follow their zigzag paths. As we observe in our simulations, the motion of

the red particles approximately approaches a mean drift velocity  $v_x \approx (dw_x/dt)/\tau$ , where  $\tau = (1 + \sqrt{5})/2$  is the number of the golden mean. Similarly, for a phasonic drift in  $y$ -direction with  $dw_y/dt < V_0/(2\gamma a_V)$ , all particles follow the trajectories of the minima and the mean drift is smaller than  $(dw_y/dt)/\tau$ . However, for  $dw_y/dt > V_0/(2\gamma a_V)$ , the net colloidal drift is  $(dw_y/dt)/\tau$ . The increase is due to the fact that the particles depicted brown in fig. 1(b) no longer follow the motion of the minimum while the magenta colloids still obey the trajectories of the potential wells.

If the phasonic drift velocity is increased even further, we find that as soon as almost all particles cannot follow the motion of the minima, the direction of the net colloidal drift is reversed. Interestingly, in case of non-zero temperature the reversal of the drift direction occurs at larger phasonic drift velocities than for  $T = 0$ .

Figure 4(b) shows the direction of the mean colloidal drift depending on the direction of the phasonic drift. The direction of the colloidal and phasonic drift are given by the angles  $\alpha_v$  and  $\alpha_w$ , respectively, that are measured with respect to the  $y$ -direction. We find that the directions are close to  $\alpha_v = -3\alpha_w$  (blue line in fig. 4(b)). We observe that there are deviations because the colloidal drift for a phasonic drift along the symmetry axes, *i.e.* along  $(\cos[j\pi/5], \sin[j\pi/5])$  with  $j = 1 \dots 10$ , is smaller than the mean drift of particles for a phasonic drift along other directions.

## 4 Light-induced colloidal quasicrystals subjected to phasonic distortions

So far we have studied the behavior of non-interacting colloidal particles which corresponds to an ensemble of single colloids. In the following we study the dynamics within a light-induced colloidal quasicrystal for colloids that interact according to the pair potential of eq. (3).

### 4.1 Relaxation after an instantaneous phasonic displacement

We first consider the case where the substrate of a laser-induced colloidal quasicrystal undergoes an instantaneous phasonic displacement  $\Delta w_x$ . Right after the potential is changed, the quasicrystalline order of the colloids is no longer stabilized by the substrate. To quantitatively study this behavior, we calculate the bond orientational order parameter  $\Psi_{10}$  given in eq. (4). Figure 5 shows that  $\Psi_{10}$  decreases until a time of about  $0.01\beta\gamma a_V^2$ . However, after this time, the colloidal particles reorganize to the new substrate and the quasicrystalline order is reconstituted.

Interestingly, for  $\Delta w_x \leq 0.3a_V$  the minimal value of  $\Psi_{10}$  decreases for increasing  $\Delta w_x$  as shown by the blueish curves in fig. 5. However, for  $\Delta w_x \geq 0.4a_V$  the quasicrystalline order is less affected if  $\Delta w_x$  is further increased (yellow, orange, and red curve). Due to a phasonic displacement some minima that were occupied by colloids

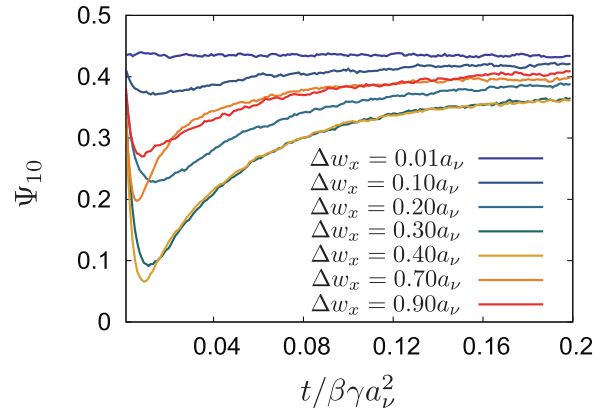


**Fig. 5.** Bond orientational order parameter  $\Psi_{10}$  as a function of time  $t/(\beta\gamma a_V^2)$  after the substrate was changed by the phasonic displacement  $\Delta w_x$ . The strength of the potential is  $\beta V_0 = 10$  and the density is chosen such, that in a triangular lattice with the same density the distance between particles is  $a_S = 0.67a_V$ , meaning that the system is in the quasicrystalline phase [13]. For  $\Delta w_x \leq 0.3a_V$  (curves with bluish colors) the minimal value of  $\Psi_{10}$  decreases for increasing  $\Delta w_x$ . For  $\Delta w_x \geq 0.4a_V$  (yellow, orange, and red curve) the minimal value of  $\Psi_{10}$  increases if  $\Delta w_x$  is further increased. The curves are averaged over 100 relaxation processes of systems with 530 colloids.

before the phasonic displacement disappear and the corresponding colloidal particle has to relax into a new potential well. As we have shown in [6] for a phasonic displacement of about  $0.4a_V$  all colloids have to slide into new minima. However, for even larger phasonic displacements it is more likely that a potential well in the new substrate is very close to the position of the old minimum and thus the quasicrystalline order is restored faster. Therefore, the quasicrystalline order of the colloids is most affected by a phasonic displacement of about  $0.4a_V$ . This result might be also important for adatoms on the surface of quasicrystals (for a review about such systems see, *e.g.*, [32]). Phasonic modes in a quasicrystal are excited by thermal energy, and therefore the amplitude of phasonic fluctuations depends on temperature. Our results suggest that quasicrystalline order of adatoms is suppressed when thermally induced phasonic fluctuations occur with a specific amplitude at a well-defined temperature. However, an increase or decrease of temperature might help to recover quasicrystalline symmetry in a monolayer of adatoms.

### 4.2 Phasonic drift-induced melting

If a laser-induced colloidal quasicrystal is subjected to a phasonic drift, the quasicrystalline order is distorted and disappears if the colloids cannot follow the changes of the substrate. In fig. 6 the pair distribution function  $g(x, y)$  for different constant phasonic drifts is displayed. For increasing phasonic drift velocity the peaks of  $g(x, y)$  broaden along the directions where colloids slide according to [6]. If the phasonic drift velocity is further increased, the quasicrystalline structure is lost. In case of a phasonic drift in the  $x$ -direction (left column in fig. 6),  $g(x, y)$  is anisotropic.

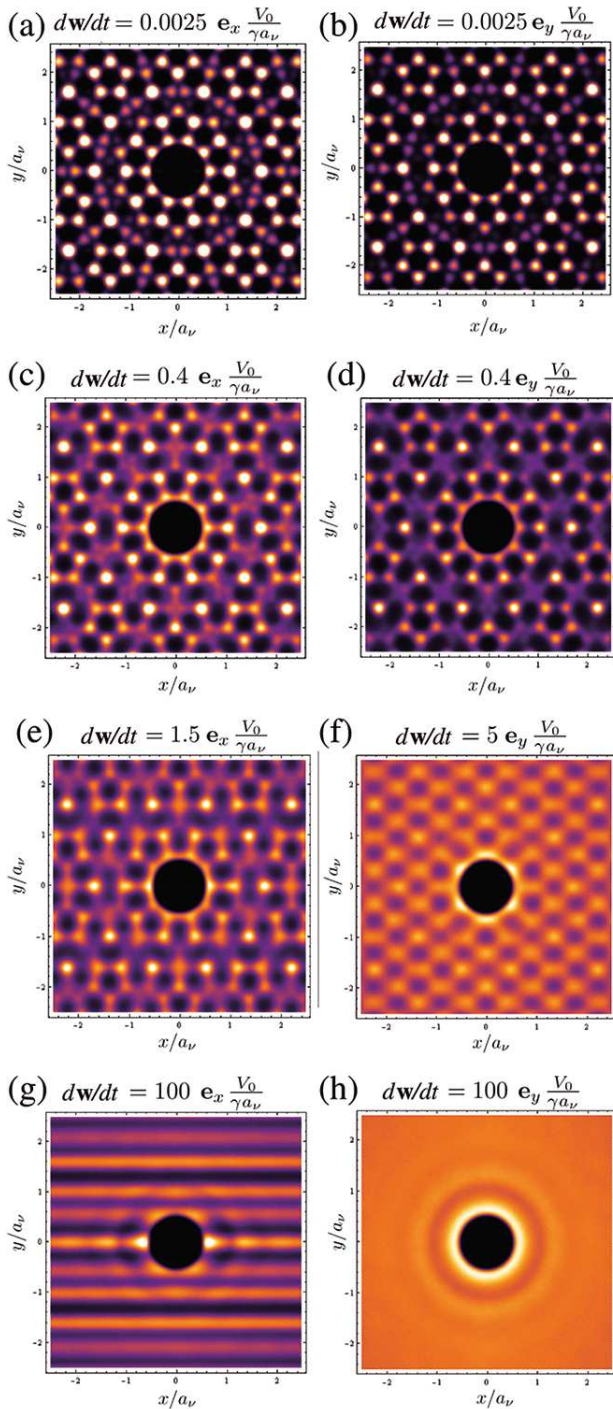


**Fig. 6.** Pair distribution function  $g(x, y)$  for colloidal quasicrystals on substrates subjected to phasonic drifts in the  $x$ -direction (left column) or  $y$ -direction (right column). The strength of the potential is  $\beta V_0 = 20$  and the density is chosen such that in a triangular lattice with the same density the distance between particles is  $a_S = 0.69a_V$ . Therefore, the system without phasonic drift is deep in the quasicrystalline phase [13]. To ensure that the system is in the steady state, we first let the colloids adjust to the phasonic drift over a time of  $100\beta\gamma a_V^2$ . Afterwards, each pair distribution function is averaged over 5000 configurations determined during a time of  $5\beta\gamma a_V^2$ . The system contains 563 particles.

For large phasonic drift velocities in the  $x$ -direction the substrate effectively corresponds to a potential  $\langle V \rangle_{w_x}$  that is averaged over  $w_x$ . As shown in [15]  $\langle V \rangle_{w_x} = \langle V \rangle_x$ , *i.e.* the effective potential no longer depends on  $x$  but only on  $y$ . Therefore, for large phasonic drift velocities in  $x$ -direction the substrate effectively corresponds to a stripe pattern oriented in the  $x$ -direction and as a consequence  $g(x, y)$  consists of such stripes (cf. fig. 6(g)) whereas the quasicrystalline order along the  $y$ -direction is not affected. For phasonic drifts in the  $y$ -direction (right column in fig. 6) no stripe pattern in  $g(x, y)$  can be observed at any phasonic drift velocity. For very large phasonic drift velocities, the colloidal particles are disordered as can be seen by the liquid-like  $g(x, y)$  in fig. 6(h). Therefore, there is a difference between a phasonic drift in the  $x$ -direction and the one in the  $y$ -direction. Here the  $x$ -direction corresponds to a symmetry direction, which is preserved by the phasonic drift. In general, a phasonic drift along any of the main symmetry axes with  $\alpha_w = j\pi/5 - \pi/2$  for an integer  $j$ , leads to a stripe-modulated fluid phase. In contrast a phasonic drift in other directions destroys the quasicrystalline structure completely.

## 5 Conclusions

We studied the behavior of colloidal particles on substrates with quasicrystalline symmetry when a phasonic displacement or drift is applied.

The mean square displacement of non-interacting colloids on a substrate with phasonic drift qualitatively is similar to the one of particles in a random potential where the depth of the minima changes randomly in time. However, there is also a mean drift motion of the colloids that cannot be explained by random potentials. The direction and velocity of the induced colloidal drift depends on the phasonic drift velocity compared to the velocity scale  $V_0/(\gamma a_V)$  given by the friction  $\gamma$ , the potential strength  $V_0$  and length scale  $a_V$ . For small phasonic drift velocities, small friction, or large potential strength, the colloids are able to follow the motion of the potential wells. However, if the phasonic drift is increased, the particles no longer remain trapped in the minima of the potential. There even is a reversal of the direction of the net colloidal drift.

A phasonic drift also changes the quasicrystalline order of a laser-induced colloidal quasicrystal. If the phasonic drift is along a symmetry direction of the quasicrystalline substrate, the quasicrystalline order is destroyed in one direction while it survives in the perpendicular direction. Other phasonic drifts affect all directions of the quasicrystal, *i.e.*, the colloidal quasicrystal is transformed into an isotropic disordered state.

The relaxation process after an instantaneous phasonic displacement depends on the amplitude of the phasonic displacement. A phasonic displacement of about  $0.4a_V$  has the most severe consequences for the colloidal quasicrystal while for a smaller or larger phasonic displacement the quasicrystalline order of the particles is less affected.

Our results are important to achieve a deeper insight into the fundamental properties of phasonic displacements

and drifts in quasicrystals. For future work it would be interesting to compare the induced phasonic drifts and fluctuations to thermally excited phasons in intrinsic quasicrystals (as for example in [33]). The colloidal system can be seen as a model system to understand the dynamics of adatoms on quasicrystalline surfaces. However, controlling colloidal motion in external fields with quasicrystalline symmetry also is important for applications with colloidal systems, like for example the growth of photonic (quasi-)crystals. Furthermore, phasonic drifts or fluctuations might also become important in other systems with decagonal symmetry, *e.g.*, for cold atoms or even Bose-Einstein condensates that are studied with optical traps with quasicrystalline symmetry [34, 35].

We thank T. Bohlein and C. Bechinger for helpful discussions and the Deutsche Forschungsgemeinschaft (DFG) for financial support (Ro 924/5). J.K. was also supported by the International Research Training Group IRTG 1740, M.S. by the DFG within the Emmy Noether programme (Schm 2657/2) and the SFB TR6.

## References

1. D. Shechtman, I. Blech, D. Gratias, J.W. Cahn, *Phys. Rev. Lett.* **53**, 1951 (1984).
2. D. Levine, P.J. Steinhardt, *Phys. Rev. Lett.* **53**, 2477 (1984).
3. D. Levine, T.C. Lubensky, S. Ostlund, S. Ramaswamy, P.J. Steinhardt, J. Toner, *Phys. Rev. Lett.* **54**, 1520 (1985).
4. C.L. Henley, M. de Boissieu, W. Steurer, *Philos. Mag.* **86**, 1131 (2006).
5. M. de Boissieu, *Isr. J. Chem.* **51**, 1292 (2011).
6. J.A. Kromer, M. Schmiedeberg, J. Roth, H. Stark, *Phys. Rev. Lett.* **108**, 218301 (2012).
7. M. Sandbrink, M. Schmiedeberg, *Aperiodic Crystals*, edited by S. Schmid, R.L. Withers, R. Lifshitz (Springer, Berlin, 2013)
8. H. Löwen, *J. Phys.: Condens. Matter* **13**, R415 (2001).
9. A. Ashkin, *Phys. Rev. Lett.* **24**, 156 (1970).
10. A. Ashkin, *Science* **210**, 1081 (1980).
11. M.M. Burns, J.M. Fournier, J.A. Golovchenko, *Science* **249**, 749 (1990).
12. M. Schmiedeberg, J. Roth, H. Stark, *Phys. Rev. Lett.* **97**, 158304 (2006).
13. M. Schmiedeberg, H. Stark, *Phys. Rev. Lett.* **101**, 218302 (2008).
14. J. Mikhael, J. Roth, L. Helden, C. Bechinger, *Nature* **454**, 501 (2008).
15. M. Schmiedeberg, J. Mikhael, S. Rausch, J. Roth, L. Helden, C. Bechinger, H. Stark, *Eur. Phys. J. E* **32**, 25 (2010).
16. J. Mikhael, G. Gera, T. Bohlein, C. Bechinger, *Soft Matter* **7**, 1352 (2011).
17. M. Schmiedeberg, J. Roth, H. Stark, *Eur. Phys. J. E* **24**, 367 (2007).
18. C. Reichhardt, C.J. Olson Reichhardt, *Phys. Rev. Lett.* **106**, 060603 (2011).
19. T. Bohlein, C. Bechinger, *Phys. Rev. Lett.* **109**, 058301 (2012).
20. C. Reichhardt, C.J. Olson Reichhardt, *J. Phys.: Condens. Matter* **25**, 225702 (2012).
21. J. Mikhael, M. Schmiedeberg, S. Rausch, J. Roth, H. Stark, C. Bechinger, *Proc. Natl. Acad. Sci.* **107**, 7214 (2010).
22. M. Schmiedeberg, H. Stark, *J. Phys.: Condens. Matter* **24**, 284101 (2012).
23. T. Bohlein, J. Mikhael, C. Bechinger, *Nat. Mater.* **11**, 126 (2012).
24. S.P. Gorkhali, J. Qi, G.P. Crawford, *J. Opt. Soc. Am. B* **23**, 149 (2006).
25. B.V. Derjaguin, L. Landau, *Acta Physicochim. (USSR)* **14**, 633 (1941).
26. E.J. Verwey, J.T.G. Overbeek, *Theory of the Stability of Lyophobic Colloids* (Elsevier, Amsterdam, 1948).
27. P. Hänggi, P. Talkner, M. Borkovec, *Rev. Mod. Phys.* **62**, 251 (1990).
28. P. Reimann, C. Van den Broeck, H. Linke, P. Hänggi, J.M. Rubi, A. Pérez-Madrid, *Phys. Rev. E* **65**, 031104 (2002).
29. C. Lutz, M. Reichert, H. Stark, C. Bechinger, *Europhys. Lett.* **74**, 719 (2006).
30. R.D.L. Hanes, C. Dalle-Ferrier, M. Schmiedeberg, M.C. Jenkins, S.U. Egelhaaf, *Soft Matter* **8**, 2714 (2012).
31. C. Emary, R. Gernert, S.H.L. Klapp, *Phys. Rev. E* **86**, 061135 (2012).
32. R. McGrath, J. Ledieu, E.J. Cox, R.D. Diehl, *J. Phys.: Condens. Matter* **14**, R119 (2002).
33. M. Engel, M. Umezaki, H.-R. Trebin, T. Odagaki, *Phys. Rev. E* **82**, 134206 (2010).
34. L. Guidoni, B. Débret, A. di Stefano, P. Verkerk, *Phys. Rev. A* **60**, R4233 (1999).
35. L. Sanchez-Palencia, L. Santos, *Phys. Rev. A* **72**, 053607 (2005).